Reaction Rate Constant of CH2O + H = HCO + H−2 Revisited: A Combined Study of Direct Shock Tube Measurement and Transition State Theory Calculation

ARTICLE *in* THE JOURNAL OF PHYSICAL CHEMISTRY A · OCTOBER 2014

Impact Factor: 2.69 · DOI: 10.1021/jp5085795 · Source: PubMed

4 AUTHORS, INCLUDING:

Shengkai Wang
Stanford University
14 PUBLICATIONS **88** CITATIONS

SEE PROFILE

THE JOURNAL OF PHYSICAL CHEMISTRY A

Article

pubs.acs.org/JPCA

Reaction Rate Constant of $CH_2O + H = HCO + H_2$ Revisited: A Combined Study of Direct Shock Tube Measurement and Transition State Theory Calculation

Shengkai Wang,[†] Enoch E. Dames,[‡] David F. Davidson,*[,†] and Ronald K. Hanson[†]

[†]High Temperature Gasdynamics Lab, Mechanical Engineering, Stanford University, Stanford, California 94305 United States

[‡]Department of Chemical Engineering, Massachusetts Institute of Technology, Cambridge, Massachusetts 02139 United States

ABSTRACT: The rate constant of the H-abstraction reaction of formaldehyde (CH_2O) by hydrogen atoms (H), $CH_2O + H = H_2 + HCO$, has been studied behind reflected shock waves with use of a sensitive mid-IR laser absorption diagnostic for CO, over temperatures of 1304−2006 K and at pressures near 1 atm. C_2H_5I was used as an H atom precursor and 1,3,5-trioxane as the CH_2O precursor, to generate a well-controlled CH_2O/H reacting system. By designing the experiments to maintain relatively constant H atom concentrations, the current study significantly boosted the measurement sensitivity of the target reaction and suppressed the influence of interfering reactions. The measured $CH_2O + H$ rate constant can be expressed in modified Arrhenius from as $k_{CH_2O+H}(1304-2006\ K, 1\ atm) = 1.97 \times 10^{11}(T/K)^{1.06} \exp(-3818\ K/T)\ cm^3\ mol^{-1}s^{-1}$, with uncertainty limits estimated to be +18%/−26%. A transition-state-theory (TST) calculation, using the CCSD(T)-F12/VTZ-F12 level of theory, is in good agreement with the shock tube measurement and extended the temperature range of the current study to 200−3000 K, over which a modified Arrhenius fit of the rate constant can be expressed as $k_{CH_2O+H}(200-3000\ K) = 5.86 \times 10^3(T/K)^{3.13} \exp(-762\ K/T)\ cm^3\ mol^{-1}\ s^{-1}$.

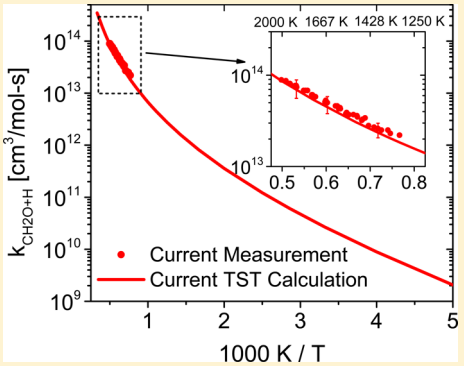

1. INTRODUCTION

Formaldehyde (CH_2O) is an important species in the combustion chemistry of hydrocarbon fuels.[1] It lies on the primary oxidation pathways of methane and methyl radical,[2,3] and plays a critical role in the conversion of carbon to CO, the oxidation of which corresponds to the majority of heat release in most hydrocarbon combustion systems.[4] Research has also shown that formaldehyde is related to cool flame phenomena and NTC behavior;[5−7] both are very important in low temperature fuel combustion chemistry. Formaldehyde is also a direct product during the pyrolysis of alcohols, ethers, and esters, including some of the popular bioderived oxygenated fuels such as butanol and methyl esters.[8−10] However, despite the abundance of formaldehyde produced in the combustion of most fuels, especially during the preignition processes, it is typically an undesired combustion product. In fact, formaldehyde is a primary vehicle emission control target for land transportation.[11] It is also a benchmark species in engine design and testing, since high levels of formaldehyde in the exhaust can be a warning of abnormal reaction quenching, or a sign of engine malfunction. Therefore, for combustion research, understanding CH_2O chemistry, and especially CH_2O removal chemistry, has great importance in both theoretical studies and practical applications.

Under the typical radical rich conditions of hydrocarbon combustion, CH_2O is mainly formed via the reaction of methyl radical with atomic oxygen, and depleted through the subsequent H-abstraction reactions of H, OH, O, and CH_3.[2,12,13] Among these aldehyde removal channels, $CH_2O + H$, $CH_2O + OH$, and $CH_2O + M$ are major contributors, in descending order. Recently, studies for the reaction rates of $CH_2O + OH$ and $CH_2O + M$ have been conducted at Stanford,[13−16] and the results are in good agreement with most previous studies. However, there is still large uncertainty in the reaction rate of $CH_2O + H$, and literature values are seen to scatter over an order of magnitude at high temperatures.[17−25] According to the comprehensive review and evaluation by Baulch et al.,[25] the experimental study from Friedrichs et al.[21] has been considered the most accurate over 1510−1960 K, though yielding results that are significant higher than most of other studies. Friedrichs et al.[21] inferred the $CH_2O + H$ rate constant from VUV absorption of CH_2O behind reflected shock waves, using C_2H_5I as the H source. Yet the nonmonochromatic nature of the VUV lamp, the relatively weak absorption of CH_2O, and the nontrivial interference absorption from other species posed significant challenges, limiting the minimum CH_2O loading to 1000 ppm.[21] As a result, the consequent uncertainties have been relatively large (2σ uncertainty factor = 1.66) in the measured rate constant. Most recently, a sensitive and interference-free mid-IR laser

Received: August 25, 2014
Revised: October 14, 2014

   dx.doi.org/10.1021/jp5085795 | J. Phys. Chem. A XXXX, XXX, XXX−XXX

absorption diagnostic for CO has been developed at Stanford that can circumvent these past challenges and difficulties and open up new alternatives for kinetics measurements.[26] Such a diagnostic has been successfully demonstrated in several recent rate constant measurements.[10,27,28] Now, with its application becoming mature, it is time to revisit the important reaction of $CH_2O + H$.

Theoretical calculations provide an alternative way to determine fundamental reaction rate constants. However, for the rate of $CH_2O + H$ the theoretical results have been sparse in the literature. Harding and Schatz performed a variety of valence bond calculations (e.g., generalized valence bond and polarization configuration interaction) to obtain the barrier height for this reaction, finding their results to vary between 12.7 and 24 kcal/mol.[29] The authors acknowledge based on past experience that the relatively more accurate polarization configuration interaction computed barrier of 12.7 kcal/mol was probably too high by up to several kilocalories/mole. Harding and Schatz also performed TST calculations using generalized valence bond configuration interaction derived parameters, having to reduce the computed barrier height to 4.9 kcal/mol in order to reconcile the computed rates with available experimental data for the title reaction.[17,30,31]

More recently, Irdam et al. in the 1990s recomputed the potential energy surface of this system with a multireference configuration interaction scheme,[20] employing a moderately sized pVDZ basis set. The authors obtained a barrier height of 12.8 kcal/mol, still too high to fit experimental data, by about a factor of 2. It is unclear why the model chemistry chosen by the authors overestimated the computed barrier height. To obtain agreement with room temperature experimental data for the reaction in question, Irdam and co-workers adjusted the barrier to 6.6 kcal/mol. Due to the small size of this system, and great advances in theory and computational power over the last 25 years, a high-level TST calculation was recomputed in this work. As will be further discussed below, Irdam and co-workers' adjusted value compares very well with the 6.4 kcal/mol barrier computed here.

Here, a new study has been conducted to determine the rate constant of $CH_2O + H$ using both a new CO laser absorption diagnostic and high-level TST modeling, with the goal of replicating the results from previous high temperature studies,[20,21] reducing the measurement uncertainties, and extending the rate expression to a wide range of temperatures.

2. EXPERIMENTAL METHODS

The high temperature pyrolysis of CH_2O provides an ideal system for investigations on CH_2O-related reactions. There have been several shock tube studies on the thermal decomposition of CH_2O,[13,16−19,32−36] leading to the following proposed chain mechanism:

$$CH_2O + M = HCO + H + M \quad (1a)$$

$$CH_2O + M = H_2 + CO + M \quad (1b)$$

$$CH_2O + H = H_2 + HCO \quad (2)$$

$$HCO + M = H + CO + M \quad (3)$$

$$H + HCO = H_2 + CO \quad (4)$$

$$HCO + HCO = CH_2O + CO \quad (5)$$

Due to strong coupling between reactions 1 and 2, several previous attempts to probe the rate of reaction 2 by studying the direct decomposition of CH_2O faced various levels of difficulty and therefore had large uncertainties.[17−19,32,34−36] The general idea of the current measurement was to boost the sensitivity of reaction 2 with H recycling in the CH_2O pyrolysis system. The H atoms consumed in reaction 2 were recycled through reaction 3, maintaining a relatively constant H atom concentration level in the reacting system. As a result, the H-abstraction reaction becomes the dominating channel of CH_2O removal, and the competition from CH_2O thermal decomposition was significantly suppressed. To track the temporal change of the CH_2O concentration, the current study monitored the stable pyrolysis product CO, which serves to track the CH_2O concentration on nearly a 1:1 ratio, utilizing a sensitive mid-IR laser absorption diagnostic.

2.1. Stanford Shock Tube Facility. The experiment has been carried out in a 14.13 cm inner diameter high-purity shock tube at Stanford University. The shock tube has a driven section of 8.5 m, and a driver section of 3.3 m, allowing for steady test time of more than 2 ms at typical test conditions. A pair of BaF_2 windows, located 2 cm away from the endwall, enabled optical access for the laser absorption diagnostics. More details about the Stanford shock tube facilities can be found in previous Stanford works.[45,46]

2.2. The Interference-Free CO Diagnostic. The concentration of CO was monitored by using mid-IR absorption near 4.7 μm, targeting the R(13) transition of the CO fundamental band. This strong and isolated transition has been well characterized by Ren et al.[26] To access this transition, an Alpes distributed-feedback (DFB) Quantum-Cascade Laser (QCL) was used. The narrow-linewidth feature of the laser enabled use of the peak of the CO transition where any disturbance was minimized. The average line width of the laser, governed by the current noise of the laser driver ($I_{noise,rms}$ < 40 μA), was estimated to be less than 0.001 cm^{-1}, more than 2 orders of magnitude smaller than that of the CO transition; the instantaneous line width of the laser was even narrower. The wavelength of the laser was monitored with a Bristol 721 wavemeter, which had a spectral resolution of 0.002 cm^{-1}. The laser wavelength was found to be very stable, with peak-to-peak drifting of less than 0.006 cm^{-1} within 5 min. The transmitted laser light was collected with a thermoelectrically cooled Vigo detector (type PVI-2TE, bandwidth =10 MHz, active area = 3 × 3 mm). The detector signal was sampled at 2.5 MHz and recorded with a 14-bit National Instrumental digital data acquisition system. The laser intensity was seen to be stable, with peak-to-peak drifting of less than 0.4% within 5 min. Within the very short test time (2 ms) of the shock tube experiment, this laser intensity fluctuation was usually overshadowed by other noise sources, especially the beam steering noise induced by density fluctuations in the turbulent boundary layer near the shock tube wall, which typically limited the minimum detectable absorption (MDA). The MDA of this study, determined from the root-mean-square error of the transmitted laser intensity during a nonreactive shock with pure argon as test gas, was found to be less than about 0.2%. This was equivalent to a minimum detection limit of about 10 ppm of CO at typical shock conditions of 1600 K and 1 atm. The CO concentration was calculated from the Beer−Lambert relation, $I/I_0 = \exp(-\sigma_{CO}\chi_{CO}nL)$, where I and I_0 were the transmitted and incident laser intensities, measured before and after the incident shock wave arrival, respectively; σ_{CO} was the

dx.doi.org/10.1021/jp5085795 | J. Phys. Chem. A XXXX, XXX, XXX−XXX

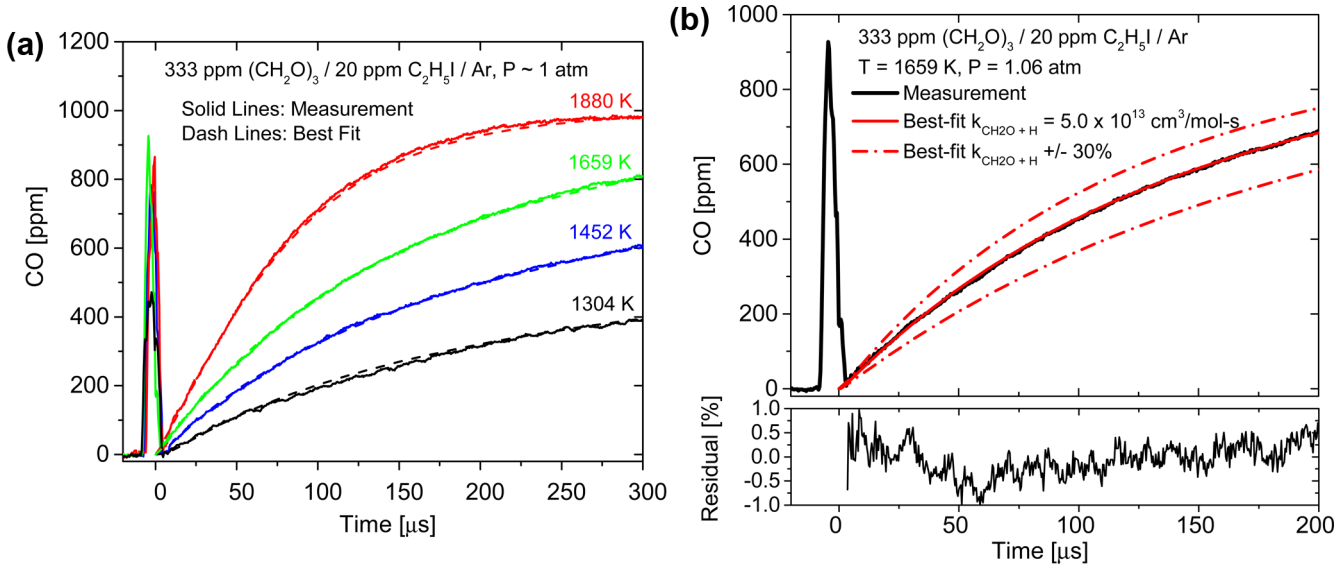

Figure 1. Example CO time-histories in the pyrolysis of the 1,3,5-trioxane/C_2H_5I/Ar mixture: (a) left panel: 4 different temperatures; and (b) right panel: 1659 K, 1.06 atm.

absorption cross section of CO, calculated using the line parameters from Ren et al.;[26] n was the total molecular number density of the shock heated gas mixture; and L was the diameter of the shock tube (14.13 cm). It is important to note that CO was the only species absorbing at the target wavelength, as was confirmed with simulations using the HITRAN 2012 spectroscopic database,[47] and with shock experiments where the laser was tuned away from the CO transition. This circumvented the difficulty of correcting for interference absorption, a challenge encountered in the previous study from Friedrichs et al.,[21] thereby improving the measurement accuracy.

2.3. H/CH_2O Sources and Gas Mixture Preparation. In this study, 1,3,5-trioxane was used as an efficient and clean precursor for CH_2O. Upon shock heating above 1050 K, 1,3,5-trioxane decomposes into three CH_2O molecules almost instantaneously.[48] More details about 1,3,5-trioxane thermal decomposition chemistry can also be found in studies of Irdam and Kiefer[49] and of Hochgreb and Dryer.[50] As mentioned above, ethyl iodide (C_2H_5I) was also introduced into the reaction system as the H atom precursor, and it underwent thermal decomposition behind the reflected shock waves via the following two reaction channels:

$$C_2H_5I = C_2H_5 + I \quad (6a)$$

$$C_2H_5I = HI + C_2H_4 \quad (6b)$$

The total rate and the branching ratio have been studied by Herzler and Frank[51] and by Kumaran et al.,[52] and recently been reevaluated by Friedrichs et al.[21] The values from Friedrichs et al.[21] have been used for the kinetics simulations in this work.

The solid-phase 1,3,5-trioxane (>99% purity), supplied by Sigma-Aldrich, was vaporized by gentle heating with warm water of 40−50 °C. This gas was then mixed with the C_2H_5I vapor, generated from its liquid form (>99% purity, also supplied by Sigma-Aldrich), and diluted in argon for use as test gas in the shock tube experiments. Prior to the mixture preparation, both 1,3,5-trioxane and C_2H_5I were purified by using a freeze−pump−thaw procedure to remove dissolved air. The bath gas argon (>99.999% purity) was supplied by Praxair and used without further purification. Gas mixtures were prepared manometrically in a 14-L stainless steel mixing tank, which was preheated to 50 °C to prevent wall condensation. The mixing tank was equipped with a magnetic stirrer, which accelerated mixing and ensured mixture homogeneity. A double-dilution method was used to allow for more accurate control of the mixture composition.[15,53] A highly concentrated mixture was first prepared and mixed for at least 2 h, and the mixture was further diluted with argon and mixed for an additional 2 h prior to experiments. Between experiments, the shock tube and the mixing assembly were routinely evacuated with a turbo-molecular pump to 6 μtorr to prevent contamination of the test mixture from any residual impurity inside the shock tube. The subsequent leak-plus-outgassing rate was less than 5 μtorr/min in these experiments.

3. MEASUREMENT RESULTS

3.1. Sample CO Time History. Figure 1a shows several representative CO time-history traces from pyrolysis experiments of 333 ppm of 1,3,5-trioxane and 20 ppm of C_2H_5I in argon. The initial distortion in the CO signals near time zero is an artifact due to deflection of the laser beam at shock wave passage, and should not be confused as a physical CO signal. Note, however, the measurement results are not influenced by this artifact despite a loss of about 5 μs test time. The time zero is determined by extrapolating the measured CO profile back to the zero level. The initial composition of the gas mixture (1000 ppm of CH_2O/20 ppm of C_2H_5I/Ar) is determined from the partial pressure of each component during the manometric preparation, and is confirmed with the CO measurement at the end of the test time. The final plateau value of CO is measured to be about 980 ppm, which agrees closely with the manometric value within measurement uncertainty. In the incident shock region before time zero, no CO formation has been observed, which is expected due to the relatively low gas temperature and pressure.

The CH_2O + H rate constant is inferred from best fitting the model prediction to match the measured CO time-history by varying the target rate constant. The mechanism used in this study is detailed in Table 1. For the particular case shown in

dx.doi.org/10.1021/jp5085795 | J. Phys. Chem. A XXXX, XXX, XXX−XXX

Table 1. Reaction Mechanism[a]

no.	reaction	A	n	E_a	ref
updated CH_2O chemistry					
1a	$CH_2O + M = HCO + H + M$[b]	3.30×10^{39}	−6.3	99.9	13
1b	$CH_2O + M = CO + H_2 + M$[b]	3.10×10^{45}	−8.0	97.5	13
2	$CH_2O + H = H_2 + HCO$	1.97×10^{11}	1.06	7.59	this study
3	$HCO + M = H + CO + M$	9.35×10^{16}	−1.00	17.0	37
4	$H + HCO = H_2 + CO$	1.20×10^{14}	0	0	37
5	$HCO + HCO = CH_2O + CO$	2.70×10^{13}	0	0	38
idoine submechanism					
6a	$C_2H_5I = C_2H_5 + I$	3.66×10^{9}	0	26.6	21
6b	$C_2H_5I = C_2H_4 + HI$	2.21×10^{7}	0	19.0	21
7	$I + CH_2O = HI + HCO$	8.32×10^{13}	0	17.4	39
8	$I + HCO = HI + CO$	5.00×10^{13}	0	0	21
9	$I + H_2 = HI + H$	2.72×10^{14}	0	33.9	40
10	$I + HI = I_2 + H$	8.02×10^{14}	0	37.1	41
11	$I + C_2H_4 = HI + C_2H_3$	1.00×10^{12}	0	6.93	21
12	$I + C_2H_2 = HI + C_2H$	1.60×10^{12}	0	17.0	21
13	$I + CH_4 = HI + CH_3$	1.48×10^{14}	0	33.0	42
14	$HI + M = H + I + M$	1.00×10^{14}	0	62.6	21
15	$I_2 + M = I + I + M$	9.79×10^{13}	0	30.4	43

[a]Rate constants are given as $k_i = AT^n \exp(-E_a/RT)$ (units kcal, cm^3, mol, s, and K). The USC Mech II mechanism serves as base mechanism.[44] Here, only those reactions are given which are not parts of the USC Mech II mechanism or which are used with a different set of rate parameters. [b]RRKM fit for T = 1400−3000 K and P = 1 bar. Collision efficiencies: M 1.0, Ar 0.7, H_2 2.0, CO 1.5, CH_2O 3.0.

Figure 1b, the residual error in the best fit is less than ±1%. Also shown are the simulated CO time-histories corresponding to the best-fit rate modified by ±30%, which indicate the very high sensitivity of CO time-history to the rate of CH_2O + H. It is also worth noting that the current study focuses on the first 200 μs of the test time, where the sensitivity of the target reaction CH_2O + H is dominant over the other reactions. This is further explained in the sensitivity analysis discussed below.

3.2. CO Sensitivity. The CO sensitivity, defined as the ratio of the percentage change in the local CO mole fraction (χ_{CO}) to the percentage change in the reaction rate under investigation (k_i), $S_{CO} = (\partial\chi_{CO}/\partial k_i)/(\chi_{CO}/k_i)$, is shown in Figure 2. The sensitivity analysis clearly indicates that the CO formation is directly related to and dominated by the target

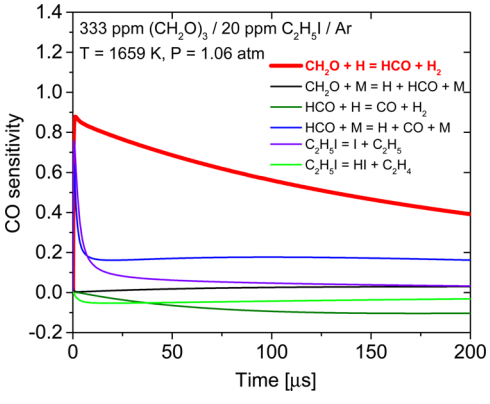

Figure 2. CO sensitivity analysis.

reaction: CH_2O + H = HCO + H_2 (reaction 2), especially during the time of interest of the current study. The reactions of HCO converting to CO, such as HCO + M = CO + H + M (reaction 3) and HCO + H = CO + H_2 (reaction 4), are typically very fast, and therefore are not rate-limiting factors in CO formation. However, these two reactions, along with the target reaction, establish quasi-equilibrium for the H concentration, and therefore influence the rate of conversion from CH_2O to CO. For example, increasing the reaction rate of HCO + M = CO + H + M by a factor of 2 would decrease the inferred CH_2O + H rate by about 23%. It is worth noting that there is large scatter for the rate constant of this reaction in the literature, among both direct measurements,[37,54−56] indirect studies,[32,57−61] and review.[62] Though lower than the values from a few indirect studies and the review from Li et al.,[32,61,62] the rate expression from the recent direct measurement of Friedrichs et al.[37] is seen to agree reasonably well with other direct measurements,[54−56] and also supports the lower range of several reported high temperature rate constants;[57,58,60] therefore it is used in the current study. More recently, the laminar burning velocity measurement and Monte Carlo rate optimization by Santner et al.[63] has suggested a reduction of the Li et al.[62] rate by about a factor of 2, which is now consistent with the result of Friedrichs et al.[37] Other reactions, such as CH_2O + M = HCO + H + M (reaction 1a) and C_2H_5I = HI + C_2H_4 (reaction 6b), have minor influence on the CO formation (changing each reaction rate by a factor of 2 would only cause less than 7% change in the inferred rate of the title reaction).

3.3. Uncertainty Analysis. An uncertainty analysis accounting for the contributions from all these reactions is detailed in Figure 3. Also shown are the contributions from

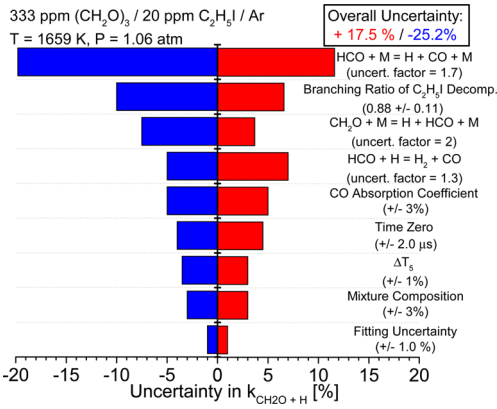

Figure 3. Uncertainty analysis for the measured rate constant of CH_2O + H.

various experimental error sources, all very small compared to the uncertainties from reaction kinetics. The predominant uncertainty source in the target rate measurement is the uncertainty in the rate of HCO + M = CO + H + M (reaction 3) (uncertainty factor = 1.7, which converts to +12%/−20% uncertainty for the target rate). However, this uncertainty can be mitigated by repeating the measurement at different C_2H_5I/CH_2O ratios, where the quasi-steady-state H concentrations are shifted to different values.

3.4. Effect of Different C_2H_5I/CH_2O Ratios. Figure 4 summarizes the target reaction rate measured at four C_2H_5I/CH_2O ratios in an Arrhenius diagram. Following the

dx.doi.org/10.1021/jp5085795 | J. Phys. Chem. A XXXX, XXX, XXX−XXX

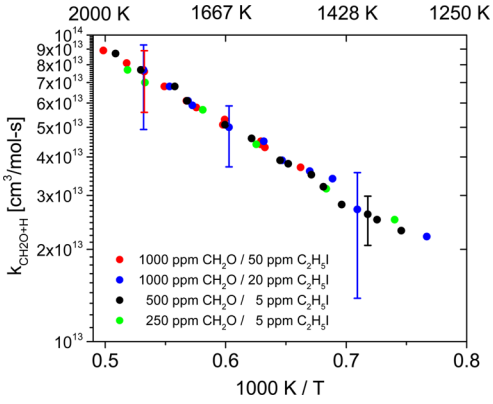

Figure 4. Rate constants of CH_2O + H measured at different mixture compositions.

uncertainty analysis mentioned above, the different choices of C_2H_5I/CH_2O ratios are optimized for different temperature regions. For example, 20 ppm of C_2H_5I/1000 ppm of CH_2O is generally good for 1500 K ≤ T ≤ 1800 K, whereas for T > 1800 K the 50 ppm of C_2H_5I/1000 ppm of CH_2O mixture yields smaller measurement uncertainty, and for T < 1500 K, 5 ppm of C_2H_5I/500 ppm of CH_2O is a better choice. Measurements have also been conducted at even lower CH_2O concentration (250 ppm) to minimize the temperature change during the pyrolysis of 1,3,5-trioxane and CH_2O (less than 5 K). Despite the variations in the uncertainty limits, all data follow the same trend and are seen to be very consistent, which is a good consistency check for the current measurement results. The lower CH_2O loading, combined with the sensitive CO diagnostic, also allows the current study to extend the rate constant data to previously inaccessible lower temperatures. A total number of 42 shocks were conducted, and the results (shown in Table 2) yield a modified Arrhenius rate expression of $k_2 = 1.97 \times 10^{11}(T/\mathrm{K})^{1.06} \exp(-3818\ \mathrm{K}/T)$ cm^3 mol^{-1} s^{-1} over 1304−2006 K.

4. TST CALCULATION

A transition state theory calculation was carried out for the H-abstraction of CH_2O by the H-radical, using the Multiwell 2014 package.[64−66] Geometries, energies, and vibrational frequencies (displayed in Table 3) were all obtained at the CCSD(T)-F12/VTZ-F12 level of theory, using the quantum chemistry package Molpro 2010.1.[67] For this model chemistry, energy convergence with basis set size may not be monatomic, thus complete basis set extrapolation is not recommended. Vibrational frequencies were not scaled. Eckart tunneling was included. Because the barrier to abstraction was determined to be 6.4 kcal/mol, a variational treatment of the transition state was not attempted. And although other possible product channels were considered, they do not compete with the H-abstraction channel and were therefore not included. For example, stabilization of the CH_3O and CH_2OH adducts, as well as the possibility for chemically activated well-skipping (i.e., $CH_2O + H \rightarrow CH_3O^* \rightarrow CH_2OH^* \rightarrow CH_2O + H$) were all considered by solving the Master Equation for energy transfer under the modified strong collider assumption using Cantherm.[68,69] For this exercise, the potential energy surface and other relevant parameters were obtained from previous work of CH_3O/CH_2OH unimolecular decomposition.[70] Rates derived from the solution of the master equation were compared with the TST rates computed here. Under the conditions of this work, the Master Equation results show negligible stabilization of CH_3O or CH_2OH compared to the rate of H-abtraction from CH_2O. The only slightly competitive channel is chemically activated well-skipping to again produce CH_2O + H. These three aforementioned channels, in comparison to the H-abstraction channel, contribute a total of 5% to the total flux at 2000 K and 1 atm. At 300 K and 1 atm, the contribution from these three channels is less than 1%. Thus, the two addition channels and well-skipping channels are neglected. The electronic energies, vibrational frequencies, and other information used in the TST calculation are presented in Table 3.

Table 2. Summary of Measured CH_2O + H Rates

T [K]	k_{CH_2O+H} [cm^3 mol^{-1} s^{-1}]
1000 ppm of CH_2O + 20 ppm of C_2H_5I	
1452	3.4×10^{13}
1493	3.6×10^{13}
1758	6.1×10^{13}
1807	6.8×10^{13}
1747	5.9×10^{13}
1880	7.7×10^{13}
1583	4.4×10^{13}
1546	3.9×10^{13}
1659	5.0×10^{13}
1304	2.2×10^{13}
1410	2.7×10^{13}
1000 ppm of CH_2O + 50 ppm of C_2H_5I	
1589	4.4×10^{13}
1581	4.3×10^{13}
1590	4.3×10^{13}
1762	6.1×10^{13}
1669	5.3×10^{13}
1510	3.7×10^{13}
1878	7.6×10^{13}
2006	8.9×10^{13}
1931	8.1×10^{13}
1821	6.8×10^{13}
1673	5.1×10^{13}
1737	5.8×10^{13}
500 ppm of CH_2O + 5 ppm of C_2H_5I	
1761	6.1×10^{13}
1966	8.7×10^{13}
1550	3.8×10^{13}
1468	3.2×10^{13}
1393	2.6×10^{13}
1436	2.8×10^{13}
1378	2.5×10^{13}
1341	2.3×10^{13}
1668	5.1×10^{13}
1609	4.6×10^{13}
1534	3.7×10^{13}
1490	3.5×10^{13}
1888	7.7×10^{13}
1793	6.8×10^{13}
250 ppm of CH_2O + 5 ppm of C_2H_5I	
1876	7.4×10^{13}
1599	4.6×10^{13}
1928	8.0×10^{13}
1463	3.3×10^{13}
1351	2.5×10^{13}

dx.doi.org/10.1021/jp5085795 | J. Phys. Chem. A XXXX, XXX, XXX−XXX

Table 3. Summary of 0 K Electronic Energies (E_0), Vibrational Frequencies, Rotational Data, and Electronic Partition Functions (Q_{el}) Used in the Transition State Calculations

species	E_0 (hartrees)	ZPE (kcal/mol)	vib freq (cm^{-1})	inactive[a] (cm^{-1})	active[b] (cm^{-1})	Q_{el}
CH_2O	−114.38146	15.51	1157.45, 1195.47, 1531.86, 1691.88, 2586.73, 2686.77	1.227	9.369	1
TS(CH_2O+H)	−114.87037	14.98	*1691.3i*, 323.58, 384.89, 1160.1, 1172.7, 1312.92, 1393.92, 1834.06, 2896.99	0.872	3.493	2
H	−0.49995	0.00				2
H_2	−1.17402	6.29	4400.94	n/a	n/a	1
HCO	−113.73017	8.17	1116.44, 1893.78, 2702.75	n/a	n/a	2

[a]Two-dimensional external rotational constants (all symmetry numbers $\sigma = 1$). [b]One-dimensional external rotational constants (symmetry number $\sigma = 1$ for TS, H, and HCO; symmetry number $\sigma = 2$ for CH_2O and H_2). [c]Not needed in TST calculations

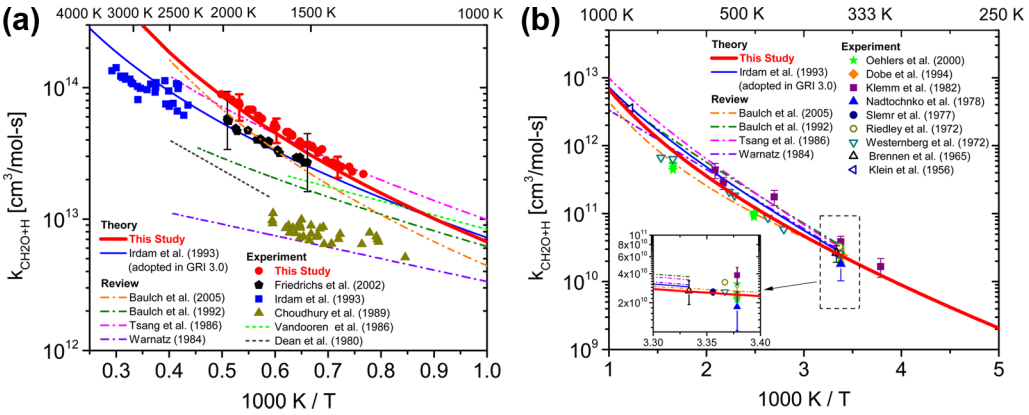

Figure 5. Arrhenius plot for the rate constant of CH_2O + H: (a) left panel: 1000−4000 K; and (b) right panel: 200−1000 K.

5. COMPARISON WITH PREVIOUS STUDIES

Figure 5a compares the target reaction rate constant from different studies at temperatures from 1000 to 2500 K. The recent shock tube study with Vis-UV CH_2O absorption by Friedrichs et al.[21] is seen to agree relatively well with the current study, within their respective error bars. The small differences between the two studies are overshadowed by the single-shot uncertainties in both data sets, which have been estimated to be ±20% for the study of Friedrichs et al.[21] and +10/−15% for the current study, comprising the uncertainties in the CH_2O and C_2H_5I concentrations, in the branching ratio of the C_2H_5I decomposition reactions, and in the fitting procedure. The minor deviation in the mean values of the two studies can possibly be explained by (1) influences from interfering absorptions and (2) different choices of the CH_2O + M = H + HCO + M (reaction 1a) rate constants. Notably, by employing a narrow line width and species-selective mid-IR laser absorption diagnostic for CO, the current study is totally free from any interference absorption; and the current rate choice for CH_2O + M = H + HCO + M (reaction 1a) has incorporated the finding from a more recent study.[13] As a result, the current study has reduced the uncertainty in the target rate constant measurement by more than half.

The earlier shock tube laser-schlieren study by Irdam et al.[20] lies above the temperature range of the current measurement, and is seen to agree in trend with the current study but with larger scatter. Irdam et al.[20] also performed a conventional TST calculation assuming an energy barrier of 6.6 kcal/mol for the transition state. That result, shown in Figure 5a, is in reasonable agreement with the current measurement and TST calculation.

The low-pressure flame study from Vandooren et al.[18] and the shock tube study from Dean et al.[17] have also yielded rate constant expressions for the target reaction, but with much higher uncertainties. The rate constant expression from Vandooren et al.[18] agrees reasonably well with the current study at lower temperatures, but begins to diverge near the high temperature limit (1500 K) of their measurement regime. The rate expression from Dean et al.[17] agrees less well with the current study. Choudhury and Lin[19] have attempted to infer the target reaction rate from shock tube measurements of methyl nitrite and 1,3,5-trioxane pyrolysis. However, due to the strong coupling between the target reaction and the thermal decomposition of CH_2O into HCO + H, the results of this measurement are less accurate and fall well below the current results.

The recommended rate expression for the target reaction from a comprehensive review on the combustion chemistry of methane and related compounds, conducted by Tsang and Hampson,[23] is seen to be in excellent agreement with the current study. The critically evaluated rate expression from the review from Baulch et al.[24] falls well below the current study but within its uncertainty limit (uncertainty factor = 3.16). A more recent work from Baulch et al.[25] has incorporated the findings of Friedrichs et al.,[21] and is seen to yield better agreement with the current study than the earlier Baulch et al.[24] review. The dated rate recommendation from Warnatz[22] was mainly based on indirect measurements prior to 1980, and is seen to be much lower than the current study.

Figure 5b compares the target reaction rate constant from different studies at temperatures from 250 to 1000 K. Notably, the current TST calculation is seen to agree well with most of the previous studies.[30,71−77] That the agreement between the TST calculation and present studies is excellent is perhaps fortuitous, but also lends credence to the high-level model chemistry employed here. To illustrate this, we note that TST calculations were originally employed using CCSD(T)-F12/

dx.doi.org/10.1021/jp5085795 | J. Phys. Chem. A XXXX, XXX, XXX−XXX

VTZ-F12 electronic energies with density functional theory (M08/MG3S) optimized geometries and frequencies. Compared to the model chemistry used in this work (energies, geometries, and frequencies all computed at the CCSD(T)-F12/VTZ-F12 level of theory) the CCSD(T)-F12/VTZ-F12//M08/MG3S derived results overestimate the rate constant at room temperature by a factor of 10, solely due to an overestimation in the two lowest vibrational modes. These lower vibrational modes are what also give high curvature to the predicted Arrhenius curve in comparison with much previous work. However, the uncertainty in the predicted rate constant is without a doubt higher than that in the experimental data, especially at lower temperatures where the influence of tunneling may not be properly captured by the Eckart approximation.

6. CONCLUSIONS

The rate constant of the H-abstraction reaction of CH_2O by H, i.e., $CH_2O + H = H_2 + HCO$, has been inferred from accurate CO time-histories in shock tube pyrolysis experiments of 1,3,5-trioxane and C_2H_5I mixtures. A modified Arrhenius equation for this reaction rate constant, valid from 1304 to 2006 K and near 1 atm, is given by $k_2 = 1.97 \times 10^{11}(T/\mathrm{K})^{1.06} \exp(-3818\ \mathrm{K}/T)$ +18/−26% $\mathrm{cm^3\ mol^{-1}\ s^{-1}}$. A complementary TST calculation has also been conducted, which strongly supports the shock tube measurements, and yielded a wide-range modified Arrhenius fit over 200−3000 K: $k_2 = 5.86 \times 10^3(T/\mathrm{K})^{3.13} \exp(-762\ \mathrm{K}/T)$ $\mathrm{cm^3\ mol^{-1}\ s^{-1}}$.

The results from both the measurement and the TST calculation have been evaluated in comparison with previous studies. At $T > 1000$ K, the values from the current study are higher than most values in the literature, but the sensitive and accurate experimental method employed yields smaller uncertainties. At $T < 1000$ K, the current rate recommendation agrees well with most of the previous low temperature studies.[30,71−77] We thus recommend our current results for future use in combustion kinetics modeling.

AUTHOR INFORMATION

Corresponding Author

*E-mail: dfd@stanford.edu. Fax: +1-(650)-723-1748.

Notes

The authors declare no competing financial interest.

ACKNOWLEDGMENTS

This material is based upon work supported by the U.S. Department of Energy, Office of Science, Office of Basic Energy Sciences, with Dr. Wade Sisk as contract monitor, under Award No. DE-FG02-88ER-13857.

REFERENCES

(1) Salooja, K. C. The Role of Aldehydes in Combustion: Studies of the Combustion Characteristics of Aldehydes and of Their Influence on Hydrocarbon Combustion Processes. *Combust. Flame* **1965**, *9*, 373−382.

(2) Warnatz, J. In *Combustion Chemistry*; Gardiner, W. C., Jr., Ed.; Springer-Verlag: New York, NY, 1984; pp 202−204.

(3) Pollard, R. T. In *Comprehensive Chemical Kinetics*; Bamford, C. H., Tipper, C. F. H., Eds.; Elsevier: New York, NY, 1977; Vol. *17*, pp 249−367.

(4) Smith, G. P.; Golden, D. M.; Frenklach, M.; Moriarty, N. W.; Eiteneer, B.; Goldenberg, M.; Bowman, C. T.; Hanson, R. K.; Song, S.; Gardiner, W. C., Jr. et al. *GRI-Mech*, Version 3.0, 1999, http://www.me.berkeley.edu/gri_mech/.

(5) Sheinson, R. S.; Williams, F. W. Chemiluminescence Spectra from Cool and Blue Flames: Electronically Excited Formaldehyde. *Combust. Flame* **1973**, *21*, 221−230.

(6) Halstead, M. P.; Prothero, A.; Quinn, C. P. Modeling the Ignition and Cool-Flame Limits of Acetaldehyde Oxidation. *Combust. Flame* **1973**, *20*, 211−221.

(7) Campbell, M. F.; Wang, S.; Christopher, G. S.; Spearrin, R. M.; Tulgestke, A. M.; Zaczek, L. T.; Davidson, D. F.; Hanson, R. K. Constrained Reaction Volume Shock Tube Study of n-Heptane Oxidation: Ignition Delay Times and Time-Histories of Multiple Species and Temperature. *Proc. Combust. Inst.* **2014**, DOI: 10.1016/j.proci.2014.05.001.

(8) McEnally, C. S.; Pfefferle, L. D. Fuel Decomposition and Hydrocarbon Growth Processes for Oxygenated Hydrocarbons: Butyl Alcohols. *Proc. Combust. Inst.* **2005**, *30*, 1363−1370.

(9) Sarathy, S. M.; Vranckx, S.; Yasunaga, K.; Mehl, M.; Oßwald, P.; Metcalfe, W. K.; Westbrook, C. K.; Pitz, W. J.; Kohse-Höinghaus, K.; Fernandes, R. X.; et al. A Comprehensive Chemical Kinetic Combustion Model for the Four Butanol Isomers. *Combust. Flame* **2012**, *159*, 2028−2055.

(10) Ren, W.; Lam, K. Y.; Pyun, S. H.; Farooq, A.; Davidson, D. F.; Hanson, R. K. Shock Tube/Laser Absorption Studies of the Decomposition of Methyl Formate. *Proc. Combust. Inst.* **2013**, *34*, 453−461.

(11) Wagner, T.; Wyszynski, M. L. Aldehydes and Ketones in Engine Exhaust Emissions—A Review. *Proc.-Inst. Mech. Eng.* **1996**, *210*, 109−122.

(12) Najm, H. N.; Paul, P. H.; Mueller, C. J.; Wyckoff, P. S. On the Adequacy of Certain Experimental Observables as Measurements of Flame Burning Rate. *Combust. Flame* **1998**, *113*, 312−332.

(13) Friedrichs, G.; Davidson, D. F.; Hanson, R. K. Validation of a Thermal Decomposition Mechanism of Formaldehyde by Detection of CH_2O and HCO behind Shock Waves. *Int. J. Chem. Kinet.* **2004**, *36*, 157−169.

(14) Vasudevan, V.; Davidson, D. F.; Hanson, R. K. Direct Measurements of the Reaction OH + CH_2O→ HCO+ H_2O at High Temperatures. *Int. J. Chem. Kinet.* **2005**, *37*, 98−109.

(15) Wang, S.; Davidson, D. F.; Hanson, R. K. High Temperature Measurements for the Rate Constants of C_1-C_4 Aldehydes with OH in a Shock Tube. *Proc. Combust. Inst.* **2014**, DOI: 10.1016/j.proci.2014.06.112.

(16) Vasudevan, V.; Davidson, D. F.; Hanson, R. K.; Bowman, C. T.; Golden, D. M. High-Temperature Measurements of the Rates of the Reactions CH_2O+ Ar → Products and $CH_2O + O_2$→ Products. *Proc. Combust. Inst.* **2007**, *31*, 175−183.

(17) Dean, A. M.; Johnson, R. L.; Steiner, D. C. Shock-Tube Studies of Formaldehyde Oxidation. *Combust. Flame* **1980**, *37*, 41−62.

(18) Vandooren, J.; de Guertechin, L. O.; Van Tiggelen, P. J. Kinetics in a Lean Formaldehyde Flame. *Combust. Flame* **1986**, *64*, 127−139.

(19) Choudhury, T. K.; Lin, M. C. Pyrolysis of Methyl Nitrite and 1,3,5-Trioxane Mixtures in Shock Waves: Kinetic Modeling of the H + CH_2O Reaction Rate. *Combust. Sci. Technol.* **1989**, *64*, 19−28.

(20) Irdam, E. A.; Kiefer, J. H.; Harding, L. B.; Wagner, A. F. The Formaldehyde Decomposition Chain Mechanism. *Int. J. Chem. Kinet.* **1993**, *25*, 285−303.

(21) Friedrichs, G.; Davidson, D. F.; Hanson, R. K. Direct Measurements of the Reaction H + CH_2O→ H_2 + HCO behind Shock Waves by Means of Vis−UV Detection of Formaldehyde. *Int. J. Chem. Kinet.* **2002**, *34*, 374−386.

(22) Warnatz, J. In *Combustion Chemistry*; Gardiner, W. C., Jr., Ed.; Springer-Verlag: New York, NY, 1984; pp 197−360.

(23) Tsang, W.; Hampson, R. F. Chemical Kinetic Data Base for Combustion Chemistry. Part I. Methane and Related Compounds. *J. Phys. Chem. Ref. Data* **1986**, *15*, 1087−1279.

(24) Baulch, D. L.; Cobos, C. J.; Cox, R. A.; Esser, C.; Frank, P.; Just, Th.; Kerr, J. A.; Pilling, M. J.; Troe, J.; Walker, R. W.; et al. Evaluated

Kinetic Data for Combustion Modelling. *J. Phys. Chem. Ref. Data* **1992**, *21*, 411−734.
(25) Baulch, D. L.; Bowman, C. T.; Cobos, C. J.; Cox, R. A.; Just, Th.; Kerr, J. A.; Pilling, M. J.; Stocker, D.; Troe, J.; Tsang, W.; et al. Evaluated Kinetic Data for Combustion Modeling: Supplement II. *J. Phys. Chem. Ref. Data* **2005**, *34*, 757−1397.
(26) Ren, W.; Farooq, A.; Davidson, D. F.; Hanson, R. K. CO Concentration and Temperature Sensor for Combustion Gases using Quantum-Cascade Laser Absorption near 4.7 μm. *Appl. Phys. B: Laser Opt.* **2012**, *107*, 849−860.
(27) Lam, K. Y.; Ren, W.; Pyun, S. H.; Farooq, A.; Davidson, D. F.; Hanson, R. K. Multi-Species Time-History Measurements during High-Temperature Acetone and 2-Butanone Pyrolysis. *Proc. Combust. Inst.* **2013**, *34*, 607−615.
(28) Ren, W.; Dames, E. E.; Hyland, D.; Davidson, D. F.; Hanson, R. K. Shock Tube Study of Methanol, Methyl Formate Pyrolysis: CH_3OH and CO Time-History Measurements. *Combust. Flame* **2013**, *160*, 2669−2679.
(29) Harding, L. B.; Schatz, G. C. An *Ab Initio* Determination of the Rate Constant for H + H_2CO→ H_2 + HCO. *J. Chem. Phys.* **1982**, *76*, 4296−4297.
(30) Klemm, B. R. Absolute Rate Parameters for the Reactions of Formaldehyde with O Atoms and H Atoms over the Temperature Range 250−500 K. *J. Chem. Phys.* **1979**, *71*, 1987−1993.
(31) Baldwin, R. R.; Cowe, D. W. The Inhibition of Hydrogen + Oxygen Reaction by Formaldehyde. *Trans. Faraday Soc.* **1962**, *58*, 1768−1781.
(32) Hidaka, Y.; Taniguchi, T.; Kamesawa, T.; Masaoka, H.; Inami, K.; Kawano, H. High Temperature Pyrolysis of Formaldehyde in Shock Waves. *Int. J. Chem. Kinet.* **1993**, *25*, 305−322.
(33) Kumaran, S. S.; Carroll, J. J.; Michael, J. V. The Branching Ratio in the Thermal Decomposition of H_2CO. *Proc. Combust. Inst.* **1998**, *27*, 125−133.
(34) Eiteneer, B.; Yu, C. L.; Goldenberg, M.; Frenklach, M. Determination of Rate Coefficients for Reactions of Formaldehyde Pyrolysis and Oxidation in the Gas Phase. *J. Phys. Chem. A* **1998**, *102*, 5196−5205.
(35) Buxton, J. P.; Simpson, C. J. S. M. The High-Temperature Pyrolysis of Formaldehyde: Kinetics and Energy Disposal to CO (v). *Chem. Phys. Lett.* **1986**, *128*, 577−582.
(36) Saito, K.; Kakumoto, T.; Nakanishi, Y.; Imamura, A. Thermal Decomposition of Formaldehyde at High Temperatures. *J. Phys. Chem.* **1985**, *89*, 3109−3113.
(37) Friedrichs, G.; Herbon, J. T.; Davidson, D. F.; Hanson, R. K. Quantitative Detection of HCO behind Shock Waves: The Thermal Decomposition of HCO. *Phys. Chem. Chem. Phys.* **2002**, *4*, 5778−5788.
(38) Temps, F.; Wagner, H. Gg. Kinetics of the Reactions of HCO with HCO and O_2. *Ber. Bunsen-Ges. Phys. Chem.* **1984**, *88*, 410−414.
(39) Walsh, R.; Benson, S. W. Kinetics and Mechanism of the Gas Phase Reaction between Iodine and Formaldehyde and the Carbon-Hydrogen Bond Strength in Formaldehyde. *J. Am. Chem. Soc.* **1966**, *88*, 4570−4575.
(40) Michael, J. V.; Kumaran, S. S.; Su, M. C.; Lim, K. P. Thermal Rate Constants over Thirty Orders of Magnitude for the I + H_2 Reaction. *Chem. Phys. Lett.* **2000**, *319*, 99−106.
(41) Garrett, B. C.; Truhlar, D. G. Generalized Transition State Theory. Canonical Variational Calculations using the Bond Energy-Bond Order Method for Bimolecular Reactions of Combustion Products. *J. Am. Chem. Soc.* **1979**, *101*, 5207−5217.
(42) Pardini, S. P.; Martin, D. S. Kinetics of the Reaction between Methane and Iodine from 830 to 1150 K in the Presence and Absence of Oxygen. *Int. J. Chem. Kinet.* **1983**, *15*, 1031−1043.
(43) Troe, J.; Wagner, H. Gg. Hochdruckverhalten der Dissoziation und Rekombination von Jod. *Z. Phys. Chem.* **1967**, *55*, 326−328.
(44) Wang, H.; You, X.; Joshi, A. V.; Davis, S. G.; Laskin, A.; Egolfopoulos, F.; Law, C. K. *USC Mech*, Version II, May 2007, http://ignis.usc.edu/USC_Mech_II.htm.
(45) Hanson, R. K.; Pang, G. A.; Chakraborty, S.; Ren, W.; Wang, S.; Davidson, D. F. Constrained Reaction Volume Approach for Studying Chemical Kinetics behind Reflected Shock Waves. *Combust. Flame* **2013**, *160*, 1550−1558.
(46) Oehlschlaeger, M. A.; Davidson, D. F.; Hanson, R. K. High-Temperature Thermal Decomposition of Isobutane and n-Butane behind Shock Waves. *J. Phys. Chem. A* **2004**, *108*, 4247−4253.
(47) Rothman, L. S.; Gordon, I. E.; Babikov, Y.; Barbe, A.; Chris Benner, D.; Bernath, P. F.; Birk, M.; Bizzocchi, L.; Boudon, V.; Brown, L. R.; et al. The HITRAN2012 Molecular Spectroscopic Database. *J. Quant. Spectrosc. Radiat. Transfer* **2013**, *130*, 4−50.
(48) Wang, S.; Davidson, D. F.; Hanson, R. K. High-Temperature Laser Absorption Diagnostics for CH_2O and CH_3CHO and Their Application to Shock Tube Kinetic Studies. *Combust. Flame* **2013**, *160*, 1930−1938.
(49) Irdam, E. A.; Kiefer, J. H. The Decomposition of 1,3,5-Trioxane at Very High Temperatures. *Chem. Phys. Lett.* **1990**, *166*, 491−494.
(50) Hochgreb, S.; Dryer, F. L. Decomposition of 1,3,5-Trioxane at 700−800 K. *J. Phys. Chem.* **1992**, *96*, 295−297.
(51) Herzler, J.; Frank, P. High Temperature Reactions of Phenylacetylene. *Ber. Bunsen-Ges. Phys. Chem.* **1992**, *96*, 1333−1338.
(52) Kumaran, S. S.; Su, M. C.; Lim, K. P.; Michael, J. V. The Thermal Decomposition of C_2H_5I. *Proc. Combust. Inst.* **1996**, *26*, 605−611.
(53) Lam, K. Y.; Davidson, D. F.; Hanson, R. K. High-Temperature Measurements of the Reactions of OH with a Series of Ketones: Acetone, 2-Butanone, 3-Pentanone, and 2-Pentanone. *J. Phys. Chem. A* **2012**, *116*, 5549−5559.
(54) Krasnoperov, L. N.; Chesnokov, E. N.; Stark, H.; Ravishankara, A. R. Elementary Reactions of Formyl (HCO) Radical Studied by Laser Photolysis—Transient Absorption Spectroscopy. *Proc. Combust. Inst.* **2005**, *30*, 935−943.
(55) Krasnoperov, L. N.; Chesnokov, E. N.; Stark, H.; Ravishankara, A. R. Unimolecular Dissociation of Formyl Radical, HCO = H + CO, Studied over 1−100 bar Pressure Range. *J. Phys. Chem. A* **2004**, *108*, 11526−11536.
(56) Timonen, R. S.; Ratajczak, E.; Gutman, D.; Wagner, A. F. The Addition and Dissociation Reaction H + CO = HCO. 2. Experimental Studies and Comparison with Theory. *J. Phys. Chem.* **1987**, *91*, 5325−5332.
(57) Cribb, P. H.; Dove, J. E.; Yamazaki, S. A Kinetic Study of the Pyrolysis of Methanol using Shock Tube and Computer Simulation Techniques. *Combust. Flame* **1992**, *88*, 169−185.
(58) Westbrook, C. K.; Creighton, J.; Lund, C.; Dryer, F. L. A Numerical Model of Chemical Kinetics of Combustion in a Turbulent Flow Reactor. *J. Phys. Chem.* **1977**, *81*, 2542−2554.
(59) Bowman, C. T. An Experimental and Analytical Investigation of the High-Temperature Oxidation Mechanisms of Hydrocarbon Fuels. *Combust. Sci. Technol.* **1970**, *2*, 161−172.
(60) Browne, W. G.; Porter, R. P.; Verlin, J. D.; Clark, A. H. A Study of Acetylene-Oxygen Flames. *Proc. Combust. Inst.* **1969**, *12*, 1035−1047.
(61) Schecker, H. G.; Jost, W. Zum Homogenen Thermischen Zerfall von Formaldehyd. *Ber. Bunsen-Ges. Phys. Chem.* **1969**, *73*, 521−526.
(62) Li, J.; Zhao, Z.; Kazakov, A.; Chaos, M.; Dryer, F. L.; Scire, J. J. A Comprehensive Kinetic Mechanism for CO, CH_2O, and CH_3OH Combustion. *Int. J. Chem. Kinet.* **2007**, *39*, 109−136.
(63) Santner, J.; Haas, F. M.; Dryer, F. L.; Ju, Y. High Temperature Oxidation of Formaldehyde and Formyl Radical: A Study of 1,3,5-Trioxane Laminar Burning Velocities. *Proc. Combust. Inst.* **2014** http://dx.doi.org/10.1016/j.proci.2014.05.014.
(64) MultiWell-2014.1 Software, 2014, designed and maintained by John R. Barker with contributors N. F. Ortiz, J. M. Preses, L. L. Lohr, A. Maranzana, P. J. Stimac, T. Lam Nguyen, and T. J. D. Kumar; University of Michigan, Ann Arbor, MI, http://aoss.engin.umich.edu/multiwell/.
(65) Barker, J. R. Multiple-Well, Multiple-Path Unimolecular Reaction Systems. I. MultiWell Computer Program Suite. *Int. J. Chem. Kinet.* **2001**, *33*, 232−245.

(66) Barker, J. R. Energy Transfer in Master Equation Simulations: A New Approach. *Int. J. Chem. Kinet.* **2009**, *41*, 748−763.
(67) Werner, H. J.; Knowles, P. J.; Manby, F. R.; Schütz, M.; Celani, P.; Korona, T.; Lindh, R.; Mitrushenkov, A.; Rauhut, G.; Shamasundar, K. R. et al. *MOLPRO*, Version 2010.1, A Package of Ab Initio Programs, 2010, http://www.molpro.net.
(68) Green, W. H.; Allen, J. W.; Bhoorasingh, P.; Buesser, B. A.; Ashcraft, R. W.; Beran, G. J.; Class, C. A.; Gao, C.; Goldsmith, C. F.; Harper, M. R. et al., Cantherm/RMGPy, 2013, http://greengroup.github.io/RMG-Py.
(69) Allen, J. W.; Goldsmith, C. F.; Green, W. H. Automatic Estimation of Pressure-Dependent Rate Coefficients. *Phys. Chem. Chem. Phys.* **2012**, *14*, 1131−1155.
(70) Dames, E. E.; Golden, D. M. Master Equation Modeling of the Unimolecular Decompositions of Hydroxymethyl (CH_2OH) and Methoxy (CH_3O) Radicals to Formaldehyde (CH_2O) + H. *J. Phys. Chem. A* **2013**, *117*, 7686−7696.
(71) Klein, R.; Scheer, M. D.; Schoen, L. J. The Pyrolysis of Formaldehyde. *J. Am. Chem. Soc.* **1956**, *78*, 50−52.
(72) Brennen, W. R.; Gay, I. D.; Glass, G. P.; Niki, H. Reaction of Atomic Hydrogen with Formaldehyde. *J. Chem. Phys.* **1965**, *43*, 2569−2570.
(73) Westenberg, A. A.; de Haas, N. Measurement of the Rate Constant of H + H_2CO → H_2 + HCO at 297−652 K. *J. Phys. Chem.* **1972**, *76*, 2213−2214.
(74) Šslemr, F.; Warneck, P. Kinetics of the Reaction of Atomic Hydrogen with Methyl Hydroperoxide. *Int. J. Chem. Kinet.* **1977**, *9*, 267−282.
(75) Nadtochenko, V. A.; Sarkisov, O. M.; Vedeneev, V. I. Study of the Reactions of the HCO Radical by the Intraresonator Laser Spectroscopy Method during the Pulse Photolysis of Acetaldehyde. *Russ. Chem. Bull.* **1979**, *28*, 605−607.
(76) Dobe, S.; Oehlers, C.; Temps, F.; Wagner, H. Gg.; Ziemer, H. Observation of an H/D-Isotope Exchange Channel in the Reaction D + H_2CO. *Ber. Bunsen-Ges. Phys. Chem.* **1994**, *98*, 754−757.
(77) Oehlers, C.; Wagner, H. Gg.; Ziemer, H.; Temps, F.; Dobe, S. An Investigation of the D/H Addition-Elimination and H Atom Abstraction Channels in the Reaction D + H_2CO in the Temperature Range 296 K ≤ T ≤ 780 K. *J. Phys. Chem. A* **2000**, *104*, 10500−10510.